Computational Studies of Aluminum Phosphate Polymorphs

Neil J. Henson and Anthony K. Cheetham*

Materials Department, University of California, Santa Barbara, California 93106

Julian D. Gale

Department of Chemistry, Imperial College, South Kensington, London SW7 2AY, UK

Received July 12, 1995. Revised Manuscript Received October 16, 1995[⊗]

Lattice energy minimization calculations have been carried out on a series of aluminum phosphate polymorphs using a formal charge shell model potential. The experimental structures are reproduced to a reasonable accuracy, especially in cases where high-quality crystallographic data are available on calcined structures. Good agreement is also found with previous calculations on these systems. In cases where the experimental methods give conflicting results regarding the space-group symmetry, calculated structures having lower symmetry than those observed in the crystallographic studies are suggested. An approximately linear dependence of lattice energy on density is observed; the computed lattice energies are found to span a range of 11.7 kJ mol^{-1} higher than berlinite, which compares to an experimentally determined range of 9.7 kJ mol^{-1}. Proton binding calculations have been performed on the structure of H-SAPO-37 to determine the most favorable proton sites. Both periodic and isolated defect cluster calculations correctly reproduce the sites which have the highest fractional occupancies in a crystallographic study.

Introduction

A large number of microporous aluminum phosphate materials ($AlPO_4$s) have been synthesized since the first examples were reported by Wilson and co-workers in 1982.[1] They exhibit a wide range of structural characteristics ranging from clathrate-type structures, in which the structure-directing agent is trapped within the aluminophosphate framework, to microporous structures similar to those shown by more traditional aluminosilicate systems. Although many $AlPO_4$ structures have direct aluminosilicate analogues, there are also a large number of unique framework types. Indeed, $AlPO_4$s and other phosphate derivatives often allow much larger ring structures to be formed, such as the 18-ring VPI-5 structure[2] and the 20-ring structure of cloverite.[3] Whether this is due to the extra stability conferred upon the structure by the Al/P alternation or is merely a consequence of the greater coordination numbers allowed by Al and other heteroatoms during the synthesis, is still open to debate. As with more traditional zeolites, framework atoms may be substituted to modify the properties of aluminum phosphates.[4,5] For example, aluminum can be replaced by transition metals to form MeAPOs, such as CoAPO-50,[6] and phosphorus can be substituted by silicon to form the acidic and catalytically active silicoaluminophosphate family (SAPO).[7] Despite their structural diversity and ease of modification, few aluminophosphates have so far found use in commercial applications, although a large number of systems have been shown to be catalytically active in important industrial processes, such as the use of $AlPO_4$-31 derivatives in the isomerization of butene.[8]

Computational approaches are being used increasingly in the study of microporous structures and in parallel with experimental measurements they can provide a valuable aid in the interpretation of results.[9−15] A large number of calculations have been performed on aluminosilicates, both using quantum mechanical approaches[16] and empirically derived force fields.[17] In the aluminophosphate area, de Man and co-workers used a partial charge rigid ion model to investigate the structure and spectra of $AlPO_4$-5[18] and also the struc-

[⊗] Abstract published in *Advance ACS Abstracts,* November 15, 1995.

(1) Wilson, S. T.; Lok, B. M.; Messina, C. A.; Cannan, T. R.; Flanigen, E. M. *J. Am. Chem. Soc.* **1982**, *104*, 1146−1147.
(2) Davis, M. E.; Saldarriaga, C.; Montes, C.; Garces, J.; Crowder, C. *Nature* **1988**, *331*, 698−699.
(3) Estermann, M.; McCusker, L. B.; Baerlocher, C.; Merrouche, A.; Kessler, H. *Nature* **1991**, *352*, 320−323.
(4) Flanigen, E. M.; Lok, B. M.; Patton, R. L.; Wilson, S. T. In Murakami, Y., Iijima, A., Ward, J. W., Eds. *New Developments in Zeolite Science and Technology*; Kodansha and Elsevier: Tokyo, 1986; pp 103−112.
(5) Lewis, J. M. O.; Price, J. B. U.S. Patent No. 4,873,390, 1989.
(6) Bennett, J. M.; Marcus, B. K. In Grobet, P. J., Mortier, W. J., Vansant, E. F., Schultz-Ekloff, G., Eds. *Innovation in Zeolite Materials Science*; Elsevier: Amsterdam, 1988; p 269.
(7) Lok, B. M.; Messina, C. A.; Patton, R. L.; Gajek, R. T.; Cannan, T. R.; Flanigen, E. M. *J. Am. Chem. Soc.* **1982**, *106*, 6092−6093.
(8) Zubowa, H.-L.; Richter, M.; Roost, U.; Parlitz, B.; Fricke, R. *Catal. Lett.* **1993**, *19*, 67.
(9) Bull, L. M.; Henson, N. J.; Cheetham, A. K.; Newsam, J. M.; Heyes, S. J. *J. Phys. Chem.* **1993**, *97*, 11776−11780.
(10) Schröder, K.-P.; Sauer, J. *J. Phys. Chem.* **1993**, *97*, 6579−6581.
(11) Catlow, C. R. A., Ed. *Modelling of Structure and Reactivity in Zeolites*; Academic Press: New York, 1992.
(12) Yashonath, S.; Santikary, P. *J. Phys. Chem.* **1994**, *98*, 6368−6376.
(13) Snurr, R. Q.; Bell, A. T.; Theodorou, D. N. *J. Phys. Chem.* **1994**, *98*, 5111.
(14) Smit, B.; Siepmann, J. I. *J. Phys. Chem.* **1994**, *98*, 8442.
(15) Henson, N. J.; Cheetham, A. K.; Gale, J. D. *Chem. Mater.* **1994**, *6*, 1647−1650.
(16) Sauer, J. *Chem. Rev.* **1989**, *89*, 199−255.
(17) Jackson, R. A.; Catlow, C. R. A. *Mol. Simul.* **1988**, *1*, 207−224.
(18) de Man, A. J. M.; Jacobs, W. P. J. H.; Gilson, J. P.; van Santen, R. A. *Zeolites*, **1992**, *12*, 816−836.

0897-4756/96/2808-0664$12.00/0

tures of $AlPO_4$-8 and VPI-5.[19] de Vos Burchart and co-workers employed a force field based on a covalent model to examine a wide range of aluminophosphates, as well as probing structures with higher coordinate aluminum.[20] Choi and co-workers used the electronegativity equalization method to derive a force field for $AlPO_4$-5;[21] however, since explicit parameters were obtained for each T−O pair, this somewhat limits the transferability of the force field to other systems. In this work we use the formal charge shell model[22] as the basis for our calculations. This force field has already been shown to give much better structural agreement with experiment for berlinite and MeAPO-36 than previous potential models and allows the flexibility of introducing heteroatom substitution in a rational way.

We consider a wide range of aluminum phosphate polymorphs, including both condensed phases and microporous structures, and perform lattice energy minimizations with symmetry constraints. For several aluminophosphates, structure determinations from powder diffraction data contradict solid-state NMR measurements, suggesting that a lower symmetry space group should have been used in the Rietveld refinement. We will assess to what extent our potential can be used to rationalize such questions by examining different space groups and checking the consistency with experimental data. As a further test of the quality of our model, calculated lattice energies will be compared to recent thermochemical measurements.[23] In the final section of this paper, we apply our potential to a system of catalytic interest and predict preferred binding sites for protons.

Methods and Models

The details of the potential model employed in the lattice energy calculations and the justification for the use of a formal charge model are fully described in a previous publication.[22] The program GULP[24] was used for all of the calculations. GULP is a general simulation program which allows both fitting and optimization of inorganic and organic crystal structures, in addition to the calculation of their properties. The program currently supports a wide range of functional forms to describe the force field. In particular, lattice energy minimization calculations can be performed that use the crystal symmetry to accelerate the calculation of energy and derivatives in an efficient manner. This has recently been demonstrated for a series of perovskite structures by Bush and co-workers.[25]

A wide range of $AlPO_4$ structures were considered in this work.[6,26−39] In most cases the crystallographic structures can be used directly as starting models, but for several structures we propose a number of hypothetical starting structures. The structure of Pluth and co-workers for $AlPO_4$-17[40] has several partially occupied sites, so a model was derived from the aluminosilicate analogue, erionite.[30] We also derived aluminophosphate models from the following aluminosilicates: $AlPO_4$-20 (siliceous sodalite[32]), $AlPO_4$-37 (siliceous faujasite[36]), and $AlPO_4$-42 (zeolite-A[39]), since the only structural data available were for their SAPO derivatives. For VPI-5, we used the structure of $AlPO_4$-54[41] as our starting point and lowered the symmetry to allow for Al/P alternation. Structures that contain Al having coordination numbers of five and six were in general omitted unless there was a trivial way to remove the extra coordinated atoms. No attempt was made to represent the template in these calculations, since our main interest was to assess the stability of the frameworks in the absence of the structure directing agent. The phonon spectra were also calculated at the Γ point to characterize each stationary point on the potential energy surface.

Results and Discussion

Structural Reproduction. When making a comparison with experimental crystallographic data, it is important to consider a number of effects. First, although the calculations represent the minimum energy structures at 0 K, the force field parameters were fitted to the room-temperature structure of berlinite,[22] so the effects of temperature are to some extent subsumed within the fitting procedure.

Second, many of the available crystal structures contain significant amounts of water which may alter the coordination environments of tetrahedral atoms in the structure; in several cases the structures are not calcined, so the template molecules are still present in the pore structure. Furthermore, a survey of the literature reveals that the quality of the crystals used in the crystallographic studies, and therefore the quality of the structural refinements, is not as high as that for many of the silica polymorphs considered previously.[15] In particular, many of the Rietveld refinements in the literature neglect Al−P alternation and some yield unreasonable bond lengths. In Table 1, we show a comparison of our calculated lattice parameters and space groups with previous computational and experimental results.

$AlPO_4$-5. There are several inconsistencies in the various experimental methods reported for the $AlPO_4$-5 structure. There have been three notable crystal-

(19) de Man, A. J. M.; van Santen, R. A.; Vogt, E. T. C. *J. Phys. Chem.* **1992**, *96*, 10460.
(20) de Vos Burchart, E.; van Bekkum, H.; van de Graaf, B.; Vogt, E. T. C. *J. Chem. Soc., Faraday Trans.* **1992**, *88*, 2761−2769.
(21) Choi, K. J.; Jhon, M. S.; No, K. T. *Bull. Korean Chem. Soc.* **1987**, *8*, 155.
(22) Gale, J. D.; Henson, N. J. *J. Chem. Soc., Faraday Trans.* **1994**, *90*, 3175.
(23) Navtrosky, A.; Petrovic, I.; Hu, Y.; Chen, C.-Y.; Davis, M. E. *Micro. Mater.* **1995**, *4*, 95−98.
(24) GULP (General Utility Lattice Program). Gale, J. D.; Royal Institution/Imperial College, U.K., 1992−1995.
(25) Bush, T. S.; Gale, J. D.; Catlow, C. R. A.; Battle, P. D. *J. Mater. Chem.* **1984**, *4*, 831.
(26) Thong, N.; Schwarzenbach, D. *Acta Crystallogr.* **1979**, *A35*, 658.
(27) Bennett, J. M.; Richardson, J. W.; Pluth, J. J.; Smith, J. V. *Zeolites*, **1987**, *7*, 160−162.
(28) Dessau, R. M.; Schlenker, J. L.; Higgins, J. B. *Zeolites*, **1990**, *10*, 522.
(29) Richardson, J. W.; Pluth, J. J.; Smith, J. V. *Acta Crystallogr.* **1988**, *B44*, 367.
(30) Schlenker, J. L.; Pluth, J. J.; Smith, J. V. *Acta Crystallogr.* **1977**, *B33*, 3265.
(31) Simmen, A.; McCusker, L. B.; Baerlocher, C.; Meier, W. M. *Zeolites*, **1991**, *11*, 654−661.
(32) Behrens, P.; van de Goor, G.; Wiebcke, M.; Braunbarth, C.; Schneider, A. M.; Felsche, J.; Engelhardt, G.; Fischer, P.; Fütterer, K.; Depmeier, W. *Proceedings of the 8th International Symposium on Molecular Recognition and Inclusion*, 1994.
(33) Parise, J. B. In Drzaj, B., Hocevar, S., Pejovnik, S., Eds., *Zeolites*; Elsevier: Amsterdam, 1985; p 271.
(34) Bennett, J. M.; Kirchner, R. M. *Zeolites*, **1992**, *12*, 338−342.
(35) Ito, M.; Shimoyama, Y.; Saito, Y.; Tsurita, Y.; Otake, M. *Acta Crystallogr.* **1985**, *C41*, 169.
(36) Hriljac, J. A.; Eddy, M. M.; Cheetham, A. K.; Donohue, J. A.; Ray, G. J. *J. Solid State Chem.* **1993**, *106*, 66−72.
(37) Wright, P. A.; Natarajan, S.; Thomas, J. M.; Bell, R. G.; Gai-Boyes, P. L.; Jones, R. H. *Angew. Chem., Int. Ed. Engl.* **1992**, 1472−1475.
(38) Kirchner, R. M.; Bennett, J. M. *Zeolites* **1994**, *14*, 253.
(39) Gramlich, V.; Meier, W. M. *Z. Kristallogr., Kristallogeom., Kristallphys., Kristallchem.* **1971**, *133*, 134.
(40) Pluth, J. J.; Smith, J. V.; Bennett, J. M. *Acta Crystallogr.* **1986**, *C42*, 283.
(41) Richardson, J. W.; Smith, J. V.; Pluth, J. J. *J. Phys. Chem.* **1989**, *93*, 8212.

Table 1. Comparison of Minimized Structures with Previous Calculations and Experiments

structure	space group	*a* (Å)	*b* (Å)	*c* (Å)	α (deg)	*β* (deg)	*γ* (deg)	rel energy[a] (kJ mol^{-1})
$AlPO_4$-5								
experiment[42]	*P*6*cc*	13.77	13.77	8.38	90.0	90.0	120.0	
experiment[43]	*P*6*cc*	13.74	13.74	8.47	90.0	90.0	120.0	
experiment[61]	*P*6*cc*	13.73	13.73	8.48	90.0	90.0	120.0	
theory (this work)	*P*6*cc*	13.83	13.83	8.55	90.0	90.0	120.0	0.92
theory (this work)	*P*31*c*	13.83	13.83	8.55	90.0	90.0	120.0	0.92
theory (this work)	*P*6	13.76	13.76	8.39	90.0	90.0	120.0	0.00
theory[18]	*P*6*cc*	14.18	14.18	8.68	90.0	90.0	120.0	
theory[18]	*Cc*	13.98	13.98	8.43	90.0	90.0	120.0	
theory[20]	*P*6	13.74	13.74	8.34	90.0	90.0	120.0	
theory[20]	*P*6*cc*	13.83	13.83	8.33	90.0	90.0	120.0	
$AlPO_4$-8								
experiment[28]	$Cmc2_1$	33.29	14.76	8.26	90.0	90.0	90.0	
experiment[62]	$Cmc2_1$	33.09	14.68	8.36	90.0	90.0	90.0	
theory (this work)	$Cmc2_1$	33.35	14.69	8.46	90.0	90.0	90.0	1.16
theory (this work)	$Pmn2_1$	33.16	14.63	8.37	90.0	90.0	90.0	0.07
theory (this work)	$P2_1$	14.63	18.10	8.36	90.0	66.2	90.0	0.0
theory[18]	$Cmc2_1$	34.27	14.76	8.26	90.0	90.0	90.0	
theory[20]	*Pmn*21	34.35	14.32	8.29	90.0	90.0	90.0	
$AlPO_4$-11								
experiment[27]	*Ima*2	18.71	13.47	8.44	90.0	90.0	90.0	
theory (this work)	*Ima*2	18.77	13.62	8.47	90.0	90.0	90.0	1.41
theory (this work)	*P*2	23.09	8.36	13.55	90.0	126.9	90.0	0.0
theory[20]	*P*2	18.36	13.5	8.29	90.0	90.0	89.79	
$AlPO_4$-18								
experiment[31]	*C*2/*c*	13.71	12.73	18.57	90.0	90.01	90.0	
theory (this work)	*C*2/*c*	13.68	12.61	18.44	90.0	89.99	90.0	
theory[20]	*C*2/*c*	13.83	12.72	18.63	90.0	89.5	90.0	
$AlPO_4$-25								
experiment[33]	*Abm*2	9.45	15.20	8.41	90.0	90.0	90.0	
theory (this work)	*Abm*2	9.56	15.35	8.53	90.0	90.0	90.0	1.88
theory (this work)	*Pca*21	9.40	15.33	8.32	90.0	90.0	90.0	0.0
theory[20]	*P*21	9.23	15.22	8.12	90.0	90.0	90.0	
VPI-5								
experiment[41]	$P6_3cm$	18.55	18.55	8.40	90.0	90.0	120.0	
experiment[63]	$P6_3cm$	18.52	18.52	8.33	90.0	90.0	120.0	
theory (this work)	$P6_3cm$	18.56	18.56	8.56	90.0	90.0	120.0	1.17
theory (this work)	$P6_3$	18.41	18.41	8.42	90.0	90.0	120.0	0.0
theory (this work)	*P*31*m*	18.56	18.56	8.56	90.0	90.0	120.0	1.17
theory[20]	*P*31*m*	18.64	18.64	8.33	90.0	90.0	120.0	
theory[20]	*P*31*m*	18.64	18.64	8.26	90.0	90.0	120.0	
theory[18]	$Cmc2_1$	19.01	19.01	8.48	90.0	90.0	120.0	

[a] Energy relative to most stable structure per tetrahedral atom.

lographic studies all of which adopted the space group *P*6*cc*. The original structure determination made by Bennett and co-workers was a single-crystal X-ray diffraction study on a sample with the tetrapropylammonium hydroxide template. Richardson and co-workers performed a neutron powder diffraction study of a calcined sample but were unable to refine Al and P sites independently.[42] Qui and co-workers solved the structure of a sample containing tetrapropylammonium fluoride from single-crystal X-ray data.[43] The crystal structure of Bennett and co-workers[42] showed three separate peaks for O(2) in the difference Fourier map, indicating some uncertainty in the position of this atom. In addition, solid-state NMR measurements[44,45] conclude that the actual space group symmetry is undoubtedly lower than that reported in the crystallographic study. Although we obtain a minimum-energy structure in the experimental *P*6*cc* space group, the calculated phonon spectrum shows nine imaginary vibrational modes. This indicates that the minimization was forced to end at a saddle point on the potential energy surface due to the symmetry constraints imposed by the space group. Similar results were obtained in previous computational studies on this system.

The existence of imaginary frequencies for a structure of a given symmetry is somewhat dependent on the force-field model used. For example, rigid ion models tend to produce higher symmetry structures, because the inclusion of polarization terms often stabilize lattice distortions. The imaginary frequencies are particularly sensitive to the oxygen polarizability. However, since the range of the values used for the polarizability is restricted by the criteria used to reproduce the structure, any shell model parameters would give qualitatively the same imaginary frequencies. Consequently, we would expect the symmetry distortions to be relatively insensitive to the potential parameters used.

To resolve the space group question, we performed additional minimizations in subgroups of *P*6*cc*. Using the *P*6 space group, we obtained a structure 0.92 kJ mol^{-1} lower in energy and having no imaginary phonon modes. This structure reproduces the cell parameters of the Bennett structure for $AlPO_4$-5 to within 1% and also gives good agreement with the transformed *P*6*cc* fractional coordinates (Table 2). The fractional coordinates of most of the atomic positions are reproduced

(42) Richardson, J. W.; Pluth, J. J.; Smith, J. V. *Acta Crystallogr.* **1987**, *C43*, 1469−1472.
(43) Qui, S. L.; Pang, W. Q.; Kessler, H.; Guth, J. L. *Zeolites* **1989**, *9*, 440−444.
(44) Peeters, M. P. J.; van de Ven, L. J. M.; de Haan, J. W.; van Hooff, J. H. C. *J. Phys. Chem.* **1993**, *97*, 9254.
(45) Demuth, D. Ph.D. Thesis, Universität Mainz, 1994.

Table 2. Comparison of Experimental and Calculated Structures for $AlPO_4$-5 in *P*6

Cell Parameters		
	experiment	calculated
a (Å)	13.726	13.758
c (Å)	8.484	8.392

Fractional Coordinates

	experiment[a]			calculated		
	x	*y*	*z*	*x*	*y*	*z*
Al(1)	0.3377	0.4577	0.5500	0.3368	0.4498	0.5500
Al(2)	0.3377	0.8800	0.0500	0.3382	0.8722	0.0493
P(1)	0.3283	0.4524	0.9220	0.3278	0.4451	0.9247
P(2)	0.3283	0.8759	0.4220	0.3298	0.8709	0.4240
O(1)	0.2137	0.4210	0.9720	0.2101	0.4154	0.9703
O(2)	0.2137	0.7927	0.4720	0.2123	0.7934	0.4823
O(3)	0.3312	0.4555	0.7500	0.3324	0.4218	0.7495
O(4)	0.3312	0.8757	0.2500	0.3393	0.8486	0.2496
O(5)	0.3584	0.3670	0.9740	0.3640	0.3746	1.0195
O(6)	0.3584	0.9914	0.4740	0.3584	0.9917	0.4126
O(7)	0.4126	0.5684	0.9860	0.4077	0.5693	0.9604
O(8)	0.4126	0.8442	0.4860	0.4120	0.8495	0.5190

Bond Lengths and Bond Angles

	expt	calcd		expt	calcd
Al(1)−O	1.710	1.722	Al−O(1)−P	150.1	144.9
Al(2)−O	1.710	1.725	Al−O(2)−P	150.1	149.1
P(1)−O	1.487	1.517	Al−O(3)−P	178.1	154.6
P(2)−O	1.487	1.516	Al−O(4)−P	178.1	154.1
			Al−O(5)−P	148.7	146.6
			Al−O(6)−P	148.7	141.8
			Al−O(7)−P	151.0	143.5
			Al−O(8)−P	151.0	146.5

[a] Fractional coordinates transformed into space group *P*6.

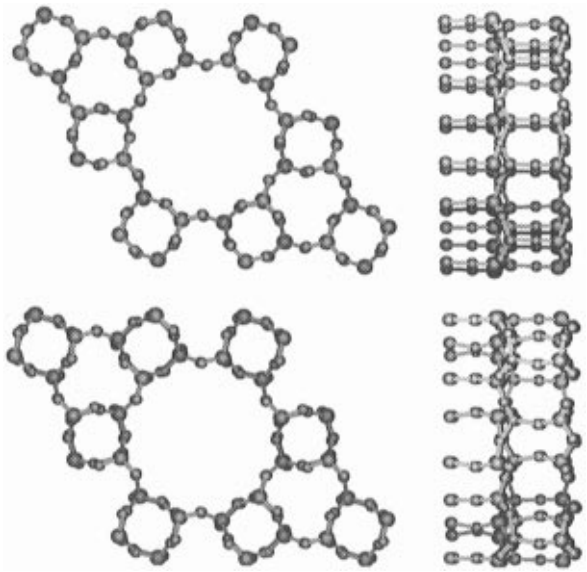

Figure 1. Comparison of experimental (top) and calculated structures of $AlPO_4$-5.

very well, the maximum shift being about 0.5 Å. The *y* coordinate of O(3) shows a shift of 0.4 Å. The range of T−O bond lengths observed is noticeably narrowed on minimization. The bond angle about O(3) (and, by symmetry, O(4)) is experimentally found to be near to 180°. This angle is reduced by about 23° during the minimization. The effect of this can be clearly seen in Figure 1. We also found that a structure minimized in the *P*3 subgroup gave a similar energy with little change in the phonon spectrum. It must be noted that the NMR studies on this system are consistent with a structure containing three distinct Al and P sites,[44,45] which is inconsistent with any of the diffraction or computational studies at this time. In keeping with the conclusion of de Man and co-workers,[18] we do not observe a layer shift on minimization with the formal charge model. However, the contention of de Man that the underestimation of the charges in their model is responsible for the stability of the structures with space group symmetry lower than experiment is not evident from our work.

$AlPO_4$-8,-11,-18, and -25. There are two structure determinations of $AlPO_4$-8 in the literature, both in space group $Cmc2_1$. Bennett and co-workers performed a time-of-flight neutron diffraction experiment,[27] whereas Dessau and co-workers used powder X-ray diffraction and a distance least-squares method to refine their model.[28] Once again, the experimental space group gave imaginary frequencies in the phonon spectrum and the space group symmetry was reduced. Two subgroups were found to give structures with no imaginary modes: $Pmn2_1$, in agreement with de Vos Burchart and co-workers, and $P2_1$, which had a significantly lower energy.

$AlPO_4$-11 also shows a deviation from the experimental space group symmetry in the minimized structure (symmetry reduced from *Ima*2 to *P*2), producing a structure that is more stable by 1.41 kJ mol^{-1}, which is consistent with the work of de Vos Burchart and co-workers.

Unlike the previous models, the energy minimization of $AlPO_4$-18 in the experimentally determined space group (*C*2/*c*) by Simmen and co-workers[31] shows no imaginary frequencies in the phonon spectrum. The three-site model is consistent with both the X-ray diffraction study and a recent NMR study.[46]

For the structure of $AlPO_4$-25, we show a deviation from the experimental space-group symmetry (*Abm*2) to lower symmetry ($Pca2_1$). The $P2_1$ model predicted by de Vos Burchart and co-workers also gives a minimized structure with no imaginary phonon modes and has the same energy as the $Pca2_1$ model.

VPI-5. Several crystallographic papers on VPI-5 are in the literature. The first was determined by Rudolph and Crowder[47] and is for a hydrated system using the space group $P6_3cm$. There is also a further structure for a hydrated sample in the lower symmetry space-group, $P6_3$,[48] featuring a helical structure of water molecules. In addition, a dehydrated structure due to Richardson and co-workers (described as $AlPO_4$-54) employs an average T-site model in the refinement (space group $P6_3$). Minimizations for the dehydrated VPI-5 structure in $P6_3cm$ yielded imaginary vibrational modes, which were eliminated on moving to the lower symmetry $P6_3$ space group. We reproduce the $AlPO_4$-54 cell parameters to within less than 1%. The larger bond angles about oxygen (>165°) are all significantly reduced in the minimized structure. NMR studies on this system[49] have been mainly concerned with the hydrated system in which one of the three Al atoms is clearly octahedrally coordinated.

Condensed Phases. In contrast to silicates, little crystallographic data exist for condensed aluminophos-

(46) He, H.; Klinowski, J. *J. Phys. Chem.* **1993**, *97*, 10385.
(47) Rudolph, P. R.; Crowder, C. E. *Zeolites*, **1990**, *1990*, *10*, 163.
(48) McCusker, L. B.; Baerlocher, C.; Jahn, E.; Bülow, M. *Zeolites* **1991**, *11*, 308−313.
(49) Davis, M. E.; Montes, C.; Hathaway, P. E.; Arhancet, J. P.; Hasha, D. L.; Garces, J. M. *J. Am. Chem. Soc.* **1989**, *111*, 3919.

Table 3. Comparison of Calculated and Experimental Structural Parameters

structure		space group	*a* (Å)	*b* (Å)	*c* (Å)	α (deg)	*β* (deg)	*γ* (deg)
berlinite[26]	expt	$P3_121$	4.94	4.94	10.94	90.0	90.0	120.0
	theory	$P3_121$	4.91	4.91	10.96	90.0	90.0	120.0
α-cristobalite[50]	expt	$C222_1$	7.09	7.09	7.00	90.0	90.0	90.0
	theory	$C222_1$	7.13	7.13	7.13	90.0	90.0	90.0
$AlPO_4$-17[30]	expt	$P6_3/m$	13.25	13.25	14.81	90.0	90.0	120.0
	theory	$P6_3/m$	13.03	13.03	15.35	90.0	90.0	120.0
$AlPO_4$-20[32]	expt	$P\bar{4}3n$	8.77	8.77	8.77	90.0	90.0	90.0
	theory	$P\bar{4}3n$	8.87	8.87	8.87	90.0	90.0	90.0
$AlPO_4$-31[34]	expt	$R\bar{3}$	20.83	20.83	5.00	90.0	90.0	120.0
	theory	$R\bar{3}$	20.65	20.65	4.99	90.0	90.0	120.0
$AlPO_4$-34[35]	expt	$R3$	13.78	13.78	14.85	90.0	90.0	120.0
	theory	$R3$	13.69	13.69	14.64	90.0	90.0	120.0
$AlPO_4$-36[37]	expt	$P\bar{1}$	13.46	22.17	5.29	90.0	92.0	90.0
	theory	$P\bar{1}$	13.16	21.51	5.16	90.0	90.9	90.0
$AlPO_4$-37[36]	expt	$Fd\bar{3}$	24.26	24.26	24.26	90.0	90.0	90.0
	theory	$Fd\bar{3}$	24.52	24.52	24.52	90.0	90.0	90.0
$AlPO_4$-41[38]	expt	$P2_1$	13.79	8.36	9.72	90.0	110.6	90.0
	theory	$P2_1$	13.59	8.33	9.70	90.0	109.2	90.0
$AlPO_4$-42[39]	expt	$Fm\bar{3}c$	17.40	17.40	42.63	90.0	90.0	120.0
	theory	$R\bar{3}c$	16.91	16.91	41.40	90.0	90.0	120.0
$AlPO_4$-46[6]	expt	$P31c$	13.23	13.23	26.89	90.0	90.0	120.0
	theory	$P31c$	13.10	13.10	26.26	90.0	90.0	120.0
$AlPO_4$-52[64]	expt	$P\bar{3}1c$	13.73	13.73	28.95	90.0	90.0	120.0
	theory	$P\bar{3}1c$	13.70	13.70	29.23	90.0	90.0	120.0
$AlPO_4$-C[65]	expt	$Pbca$	19.82	10.05	8.94	90.0	90.0	90.0
	theory	$Pbca$	19.59	10.10	8.95	90.0	90.0	90.0
$AlPO_4$-D[65]	expt	$Pca2_1$	19.19	8.58	9.80	90.0	90.0	90.0
	theory	$Pca2_1$	20.06	8.39	10.10	90.0	90.0	90.0
DAF-1[66]	expt	$P6/mcc$	22.16	22.16	42.48	90.0	90.0	120.0
	theory	$P6/mcc$	22.15	22.15	42.53	90.0	90.0	120.0

phates that possess exclusively tetracoordinate aluminum. Mooney has reported a structure for the low-temperature phase of cristobalite.[50] The minimization energy for this structure was 1.47 kJ mol^{-1} more stable than berlinite itself, which is clearly an anomalous result since berlinite is the most stable of the aluminophosphate polymorphs. We shall discuss this point further in the conclusion. Wright and Leadbetter have shown the high-temperature phase of cristobalite to have disorder on one of the oxygen sites,[51] making this structure unsuitable for consideration in this work. The remaining minimised structures are compared to experimental data in Table 3.

Variation of Lattice Energy with Density. As in our previous study of silicates,[15] the minimized lattice energy shows a roughly linear correlation with density (Figure 2). The range of energies observed from $AlPO_4$-37 to berlinite (11.7 kJ mol^{-1}) is slightly more than for the silicate analogues (10.1 kJ mol^{-1}). A recent thermochemical study[23] has measured the enthalpies relative to berlinite of several aluminophosphate structures. We show a comparison of experimental versus calculated lattice enthalpies in Table 4.

It is must be stressed here that care should be taken when making a comparison between the calculated lattice energies and the experimentally measured enthalpies. As has been mentioned earlier, since the force-field parameters have been fitted to the room-temperature structure of berlinite, the calculated internal energy has some thermal correction for structural changes due to heating. In addition, the enthalpy has a component arising from lattice vibrations. This effect could be estimated from a calculation of the heat capacity at different temperatures, as derived from the phonon spectrum, although it is likely that differences in molar quantities integrated across the phonon density of states for compounds of similar structure would be small compared to the internal energy differences.

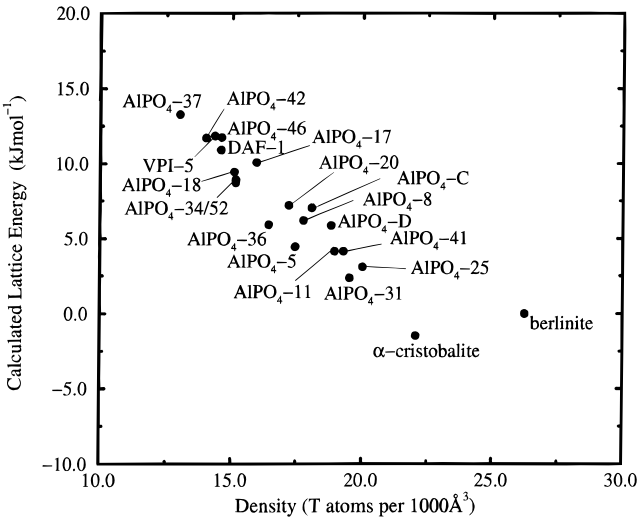

Figure 2. Calculated lattice energy as a function of density. Energy relative to berlinite per tetrahedral atom.

Table 4. Comparison of Experimental and Calculated Lattice Energies

structure	experimental lattice enthalpy[a] (kJ mol^{-1})	minimized lattice energy[a] (kJ mol^{-1})
berlinite	0.0	0.0
cristobalite	3.0	−1.6
$AlPO_4$-5	7.0	4.4
$AlPO_4$-8	5.4	6.2
$AlPO_4$-11	6.2	4.1
$AlPO_4$-42	7.8	11.7
VPI-5	9.7	10.8

[a] Relative to berlinite per tetrahedral atom.

(50) Mooney, R. C. *Acta Crystallogr.* **1956**, 728.
(51) Wright, A. E.; Leadbetter, A. *Philos. Mag.* **1975**, *31*, 1391–1401.

With these factors in mind, the agreement between experiment and theory is not as impressive as has been found in the case of silicates,[15] but the general trend of more dense structures being the most thermodynamically stable is still reproduced. The spread of calculated lattice energies is somewhat larger than experiment, probably due to the use of formal charges in the force field. Quantum mechanical calculations on silicates have shown that the actual charges are considerably less than the formal values.

Proton Sitings. One of the driving forces of the fitting of a force field for aluminophosphates using a formal charge shell model was to obtain a transferable set of potentials which were compatible with existing force fields for other systems. With this in mind, we now combine the aluminophosphate force field with that for silicates derived by Schröder and co-workers[52] to study the sitting of protons in the H-SAPO-37 system.

Schröder and co-workers have previously fitted a force field for the prediction of proton siting in aluminosilicate systems,[52] using a combination of the Sanders force field for silicates[53] and a potential for the bridging hydroxyl group derived by Saul and co-workers.[54] This force field has been used to study both the H-faujasite system[52] and H-silicalite.[55] In these studies, the interaction between the hydroxyl oxygen and adjacent T-atoms was modified to allow for the presence of the hydroxyl proton. This approach has also been adopted in this work. The primitive unit cell of SAPO-37 was constructed from the neutron diffraction study of Bull and co-workers[56] and minimized in the pure $AlPO_4$ form (final cell parameters: $a = b = c = 17.34$ Å, $\alpha = \beta = \gamma = 60.0°$). Four starting models were created by placing a proton at each of the crystallographically distinct oxygen positions in this minimized structure. The four possible proton sites are shown in Figure 3. We performed two sets of calculations on SAPO-37. The first set represents the system as periodic and consists of 24 Al species, 23 P species, one Si species, 95 oxygen species (core plus shell), and a single O−H group in the primitive unit cell of SAPO-37. Since the primitive cell dimension is 17.34 Å, interactions between protons in adjacent cells should give only a negligible perturbation to the total energy. A minimization at constant pressure was performed for each of the four possible positions for the bridging hydroxyl group. In addition to the periodic calculations, a set of defect calculations was also performed based on the approach of Mott and Littleton.[57] In this method, the proton is represented as an interstitial hydrogen atom bonded to the bridging oxygen group, the center of the defect cluster being at the silicon position. All atoms lying within a sphere of radius r_2 of the defect center are treated explicitly, and within an inner sphere of radius r_1 the atoms are allowed to relax anharmonically during the minimization. Outside the r_2 boundary, interactions with the defect are handled more approximately as a dielectric response to the defect charge. Several calculations were performed using increasing values of r_1 and r_2. Using values of $r_1 = 13$ Å and $r_2 = 24$ Å the energy change on increasing the radii further was found to be less than 0.001 eV for each minimized structure. This corresponds to an inner region of 582 atoms.

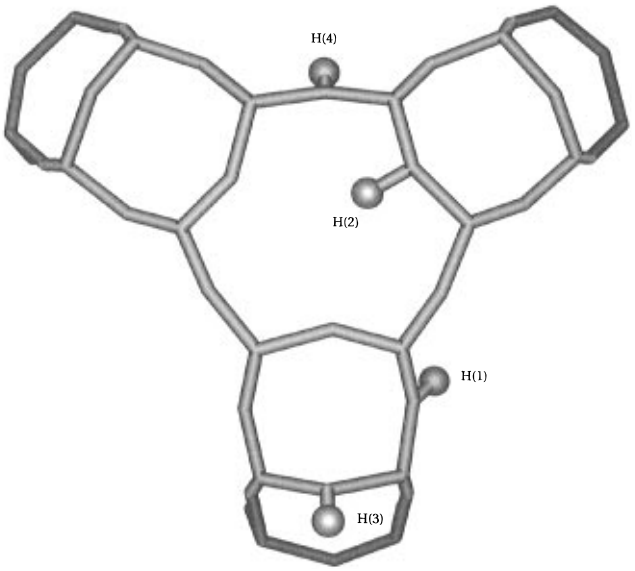

Figure 3. Possible proton positions in H-SAPO-37 using the numbering system of Bull and co-workers.[56]

Both the periodic and defect cluster calculations give the same ordering in energies, that is, decreasing stability in series O(3) ≈ O(1) ≫ O(2) > O(4). The crystallographic study of Bull and co-workers determined the proton occupancies to decrease in the order O(1) > O(2) > O(3), with no occupancy of the O(4) site. Although our calculations predict the stability of the O(1) site, the trend in the occupancies is not reproduced by the calculated proton energies. Since the crystallographic study represents an average structure with protons located at all the occupied bridging position, individual bond lengths and angles cannot be compared to our results here. In addition, since the O−H bond length was constrained to a value of 0.96 Å in the crystallographic refinement, neither can we make a direct comparison with the calculated bond length in our simulation. However, we note that the calculated values show good agreement with a recent neutron diffraction study of the proton positions in H-SAPO-34.[58]

The agreement between the structural properties for the periodic and defect calculations show the equivalence of the two approaches for this system; the discrepancies in bond lengths and bond angles being less than 0.005 Å and 0.4° (Table 5). In addition, the relative energies agree to within 0.8 kJ mol^{-1}, and the calculated O−H stretching frequencies differ by only 2 cm^{-1}. Dzwigaj and co-workers carried out IR measurements on H-SAPO-37 and found two O−H stretching frequencies at 3640 and 3575 cm^{-1}.[59] The calculated O−H stretching frequencies are too large compared to experiment. As Schröder and co-workers pointed out, the calculated vibrational frequencies with this force-field

(52) Schröder, K.-P.; Sauer, J.; Leslie, M.; Catlow, C. R. A.; Thomas, J. M. *Chem. Phys. Lett.* **1992**, *188*, 320−325.
(53) Sanders, M. J.; Leslie, M.; Catlow, C. R. A. *J. Chem. Soc., Chem. Commun.* **1984**, 1271−1273.
(54) Saul, P.; Catlow, C. R. A. *Philos. Mag. B* **1985**, *51*, 107−117.
(55) Schröder, K.-P.; Sauer, J.; Leslie, M.; Catlow, C. R. A. *Zeolites*, **1992**, *12*, 20−23.
(56) Bull, L. M.; Cheetham, A. K.; Hopkins, P. D.; Powell, B. M. *J. Chem. Soc., Chem. Commun.* **1993**, 1196.
(57) Mott, N. F.; Littleton, M. J. *J. Chem. Soc., Faraday Trans.* **1938**, *34*, 485.
(58) Smith, L. J.; Wright, P. A.; Marchese, L.; Thomas, J. M.; Cheetham, A. K., in preparation.
(59) Dzwigaj, S.; Briend, M.; Shikholeslami, A.; Peltre, M. J.; Barthomeuf, D. *Zeolites*, **1990**, *10*, 157.

Table 5. Geometries of the Four Bridging Hydroxyl Groups, Energies, and O−H Stretching Frequencies

	r_{O-H} (Å)	r_{Si-O} (Å)	r_{Al-O} (Å)	$\theta_{Al-O-Si}$ (deg)	θ_{Si-O-H} (deg)	relative energy (kJ mol^{-1})	ω (cm^{-1})
				Periodic			
O(1)	0.998	1.791	1.829	130.7	112.6	1.2	3794
O(2)	1.002	1.779	1.825	142.0	108.8	14.2	3727
O(3)	0.999	1.815	1.821	138.9	106.9	0.0	3766
O(4)	0.999	1.784	1.829	134.4	111.1	17.7	3772
				Defect Cluster			
O(1)	0.998	1.790	1.825	130.7	112.2	1.9	3792
O(2)	1.002	1.779	1.823	141.6	108.7	14.6	3728
O(3)	0.999	1.815	1.820	138.7	107.0	0.0	3765
O(4)	0.999	1.783	1.824	134.2	110.9	18.5	3770

model represent harmonic values.[52] Correcting the stretching frequency for anharmonicity corresponds to subtracting approximately 150 cm^{-1} from the calculated values, which brings them much closer to those measured by experiment. Clearly in the inability of the simulations to correctly reproduce the order of proton occupancies combined with the deficiencies in the calculated O−H frequencies suggests that further work is needed to refine the current force field.

It is interesting to note that the empirical rule relating the most favorable binding sites for protons to the bridging oxygen with the smallest angle does not appear to apply completely (see Table 6).[60] Bull and co-workers[56] have suggested that in the case of H-SAPO-37 this effect may be complicated by additional hydrogen-bonding interactions. In our minimizations, we observe that, compared to the minimized structure of the parent $AlPO_4$, the binding of the proton at the bridging causes a significant contraction in the oxygen angle. In an attempt to relate our oxygen bond angles to the crystallographic study, which essentially represents an average system with all the proton sites partially occupied, we performed two averaging schemes. In the first, we averaged the bond angles about each of the bridging oxygens over the four minimized structures, and in the second we weighted the averages with the crystallographic occupancies. The average angles from both approaches are found to reproduce the crystallographic values to within 2°, with the notable exception of the O(4) site (Table 6), which has a zero occupancy in the crystallographic structure.

Table 6. Comparison of Bond Angles about Oxygen for Experimental and Minimized Structures of SAPO-37

angle at indicated oxygen	expt[a]	minimized structures with proton at indicated site				minimized $AlPO_4$-37
		O(1)	O(2)	O(3)	O(4)	
O(1)	137.86(30)	130.7	154.7	145.4	138.7	139.6
O(2)	149.79(27)	138.5	142.0	141.6	140.1	148.4
O(3)	144.47(29)	142.6	150.8	138.9	146.3	146.9
O(4)	144.6(4)	134.4	143.6	147.2	134.4	141.6
av		136.6	147.8	143.3	139.9	
weighted av		134.1	151.5	143.7	140.1	

[a] Esd's given in parentheses.

Conclusions

We have shown that the formal charge shell model force field for aluminophosphate structures reproduces experimentally determined structures to as good an accuracy as previous force fields. In addition, the use of formal charges allows the force field to be easily extended to investigate catalytically interesting systems such as SAPOs. This work has shown that the current force field integrates well into previous approaches for studying acidity and can, to a limited extent, investigate proton sitings. However, the calculated O−H stretching frequencies and predicted energy ordering for the different sites are not satisfactory. Work is currently in progress to develop a more accurate O−H potential based on quantum mechanical calculations. The problems in correctly reproducing the structure of the condensed α-cristobalite phase suggest deficiencies in this area. One method that is being considered is to perform a simultaneous fit of the force-field parameters to both the structure of berlinite and α-cristobalite, as has been demonstrated for other ionic solids.

Acknowledgment. N.J.H. and A.K.C. thank the Science and Engineering Research Council (UK), Los Alamos National Laboratory, and Biosym Technologies, for financial support throughout this work. J.D.G. thanks the Royal Society for provision of a University Research Fellowship. This work was also supported by the UCSB-MRL under National Science Foundation Award No. DMR-9123048. We also acknowledge Dr. S. Natarajan for useful discussion.

CM9503238

(60) Gibbs, G. V.; Meagher, M. P.; Smith, J. V.; Pluth, J. J. *Mol. Sieves II* **1977**, *40*, 19.
(61) Bennett, J. M.; Cohen, J. P.; Flanigen, E. M.; Pluth, J. J.; Smith, J. V. In Stucky, G. D., Dwyer, F. G., Eds. *Intrazeolite Chemistry*, American Chemical Society: Washington, DC, 1983; p 109.
(62) Richardson, J. W.; Vogt, E. T. C. *Zeolites* **1992**, *12*, 13−19.
(63) Annen, M. J.; Young, D.; Davis, M. E.; Cavin, O. B.; Hubbard, C. R. *J. Phys. Chem.* **1991**, *95*, 1380−1383.
(64) Bennett, J. M.; Kirchner, R. M.; Wilson, S. T. In Jacobs, P. A., van Santen, R. A., Eds. *Zeolites: Facts, Figures, Future*; Elsevier: Amsterdam, 1989; p 731.
(65) Keller, E. B.; Meier, W. M.; Kirchner, R. M. *Solid State Ionics* **1990**, *43*, 93.
(66) Wright, P. A.; Jones, R. H.; Natarajan, S.; Bell, R. G.; Chen, J.; Hursthouse, M. B.; Thomas, J. M. *J. Chem. Soc., Chem. Commun.* **1993**, 633−635.